18

Anti-Stokes photoluminescence of perovskite $CsPbBr_3$ nanocrystals in a fluorophosphate glass matrix

© M.S. Kuznetsova[1], M.N. Bataev[1], M.A. Chukeev[1], N.D. Rostovtsev[1], S.Yu. Verbin[1], I.V. Ignatiev[1], V.Yu. Davydov[2], A.N. Smirnov[2], I.A. Eliseev[2], E.V. Kolobkova[3,4]

[1] Spin Optics Laboratory of St. Petersburg State University,
198504 St. Petersburg, Russia
[2] Ioffe Institute of RAS,
194021 St. Petersburg, Russia
[3] ITMO University,
199034 St. Petersburg, Russia
[4] St. Petersburg State Institute of Technology (Technical University),
190013 St. Petersburg, Russia
e-mail: mashakuznecova@bk.ru

Received September 15, 2022
Revised September 23, 2022
Accepted October 2, 2022

The anti-Stokes photoluminescence (PL) of perovskite $CsPbBr_3$ nanocrystals in a fluorophosphate glass matrix has been found and experimentally studied upon optical excitation to the low-energy edge of the photoluminescence band. The intensity of anti-Stokes PL depends linearly on the pumping power and increases rapidly with increasing temperature. A simple three-level model is proposed that describes well the main regularities of the observed phenomenon.

Keywords: perovskites, nanocrystals, anti-Stokes photoluminescence, $CsPbBr_3$, fluorophosphate glass.

DOI: 10.21883/EOS.2022.11.55108.4130-22

Introduction

Optical materials based on perovskite nanocrystals (NCs) of cesium and lead halides are promising materials for many practical applications due to their unique optical [1–3], optoelectronic [4] and photovoltaic [5] properties. To date, the prospects for the use of NCs based on $CsPbX_3$ for the creation of new laser sources [6], polarizers [7], LEDs [8], solar cells and photodetectors [9] are demonstrated. Changing the size or composition of NCs using anion and/or cation exchange [2] makes it possible to significantly vary the optical properties of these nanocrystals, expanding the range of their application.

Most of the studies were performed on colloidal perovskite NCs [1–13]. The main disadvantage of such NCs is their low resistance to the environment and high temperatures. In this regard, various types of protective coatings are used to stabilize $CsPbX_3$ [14–17]. However, these coatings are not enough to protect NCs from high temperatures. Therefore, new approaches to the creation of more stable $CsPbX_3$ NCs and the study of their optical properties are still relevant.

One of the possible ways to solve this problem is the formation of nanocrystals in glass matrices. It has been shown [18–25] that perovskite NCs in glass can be promising luminescent materials for many applications due to their strong absorption of exciting light and high luminescence quantum yield [26], which is close to quantum yield of colloidal NCs.

The choice of a fluorophosphate glass matrix for the formation of $CsPbX_3$ (X = Cl, Br, I) NCs is motivated by the possibility of introducing high concentrations of halides. Our previous studies [27–30] revealed the possibility of using fluorophosphate glasses to obtain optical materials with unique properties. In particular, they are characterized by high chemical resistance to the environment and to the action of molten salts at elevated temperatures.

In this work, we report an experimental observation of anti-Stokes photoluminescence (PL) of $CsPbBr_3$ nanocrystals in a fluorophosphate glass matrix. Upon optical excitation to the low-energy edge of the NCs PL band, an intense PL band is observed with a maximum shifted above the excitation photon energy (anti-Stokes region of the spectrum). The work proposes a simple model of the observed phenomenon.

Sample preparation technology and experimental technique

The sample under study is a fluorophosphate glass of composition $60Ba(PO_3)_2-15NaPO_3-12AlF_3-1Ga_2O_3-4Cs_2O-8PbF_2$ (mol.%) doped with 3.4 mol.% $BaBr_2$. Glass synthesis was carried out in a closed glassy carbon crucible at $T = 1000-1050^\circ$C. In our case, about 50 g of the mixed powder was melted in the crucible for 30 min. The traditional method of NC formation in glass is to obtain almost colorless transparent glass followed by long-term heat treatment at the glass transition temperature, which

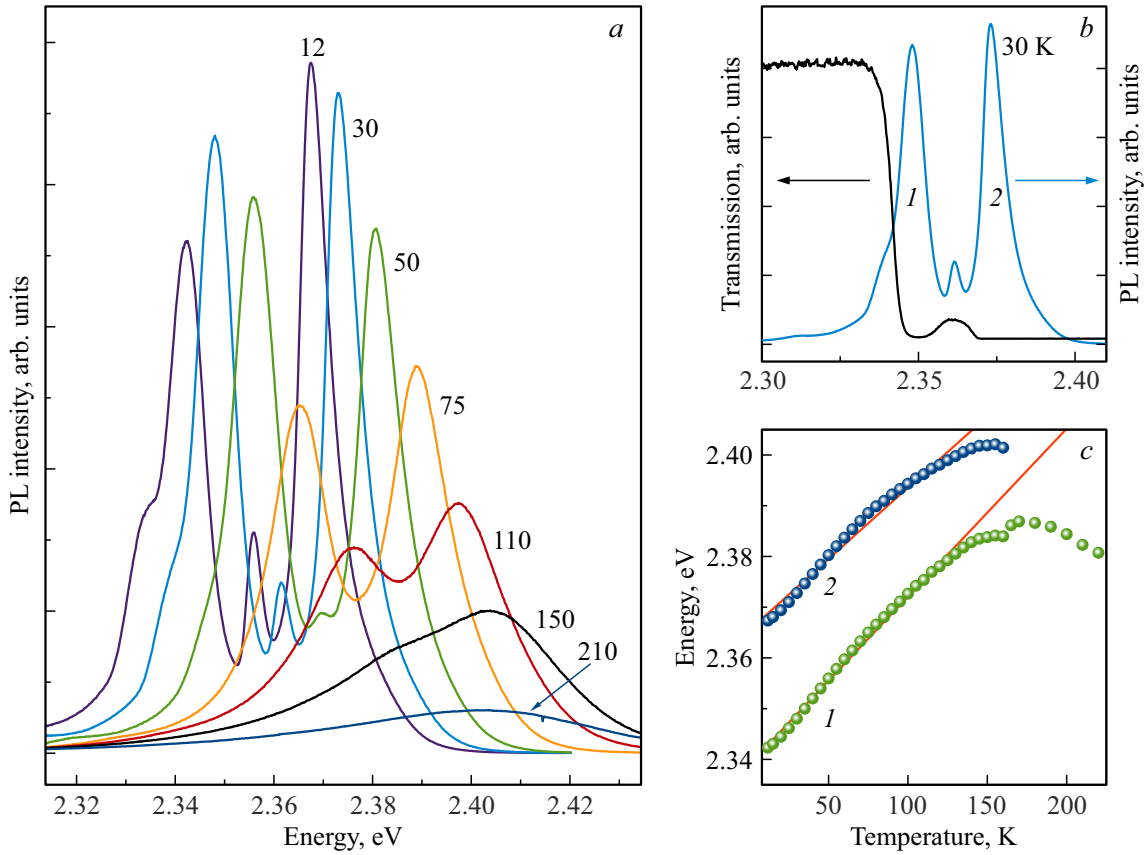

Figure 1. (*a*) PL spectra of $CsPbBr_3$ nanocrystals excited by laser radiation above the PL band ($E_{exc} = 3.06$ eV). The spectra were measured in the back scattering geometry at different sample temperatures. The temperatures are given near the curves in Kelvin. $P_{exc} = 30\,\mu$W. (*b*) PL (blue curve) and transmission (black curve) spectra measured at $T = 30$ K. (*c*) Temperature dependences of the energy of the two main PL peaks indicated in Fig. 1, *b* by numbers *1* and *2*, and their linear approximations.

was determined by STA 449F1 Jupiter Nietzsch differential scanning calorimeter and amounted to 400°C. The NCs size changed during the heat treatment. To obtain the sample for present study, heat treatment was carried out at temperature of 400°C for 240 min. The resulting glass with NCs was characterized using a X-ray diffractometer by Rigaku [26] Several weak diffraction peaks were observed in the X-ray diffraction pattern of the glass, indicating the formation of $CsPbBr_3$ crystalline phases in the glass. Analysis of the X-ray diffraction pattern made it possible to estimate the average diameter of the NCs, $d = 14.5$ nm. Similar value was obtained from an analysis of the shape and position of the PL band.

To study the PL under non-resonant excitation, it was used the standard method of stationary spectroscopy. The experimental setup is equipped with a close cycle helium cryostat, which makes it possible to vary the sample temperature in the range from 10 to 300 K. For non-resonant PL excitation, a laser with a radiation wavelength $\lambda_{exc} = 405$ nm (photon energy $E_{exc} = 3.06$ eV) was used. The laser radiation was focused into a 50-micron diaphragm and then refocused onto the sample using a short-focus lens into a spot of 40 μm in diameter. PL was collected in the back scattering geometry. The laser excitation was incident on the sample at a small angle to the optical axis so that the reflected beam did not fall into the objective aperture in the PL collection channel on the slit of the iHR-550 spectrometer (focal length 550 mm, diffraction grating 600 grooves per mm). The spectrometer is equipped with a Symphony II CCD camera cooled with liquid nitrogen, which ensures a low noise level.

To study the anti-Stokes PL, the same experimental setup was used with a slight modification. A laser with a wavelength of $\lambda_{exc} = 532$ nm ($E_{exc} = 2.33$ eV) was used as a light source, which corresponds to the long-wavelength edge of the PL band. To separate the PL signal from the scattered pumping radiation, the PL of the sample was directed to a DFS-24 double monochromator and detected by a cooled photomultiplier tube and a photon counting system.

Photoluminescence upon non-resonant excitation

The PL spectra measured under short-wavelength excitation ($\lambda_{exc} = 405$ nm, $E_{exc} = 3.06$ eV) and different temperatures are shown in Fig. 1, *a*. At a low sample temperature,

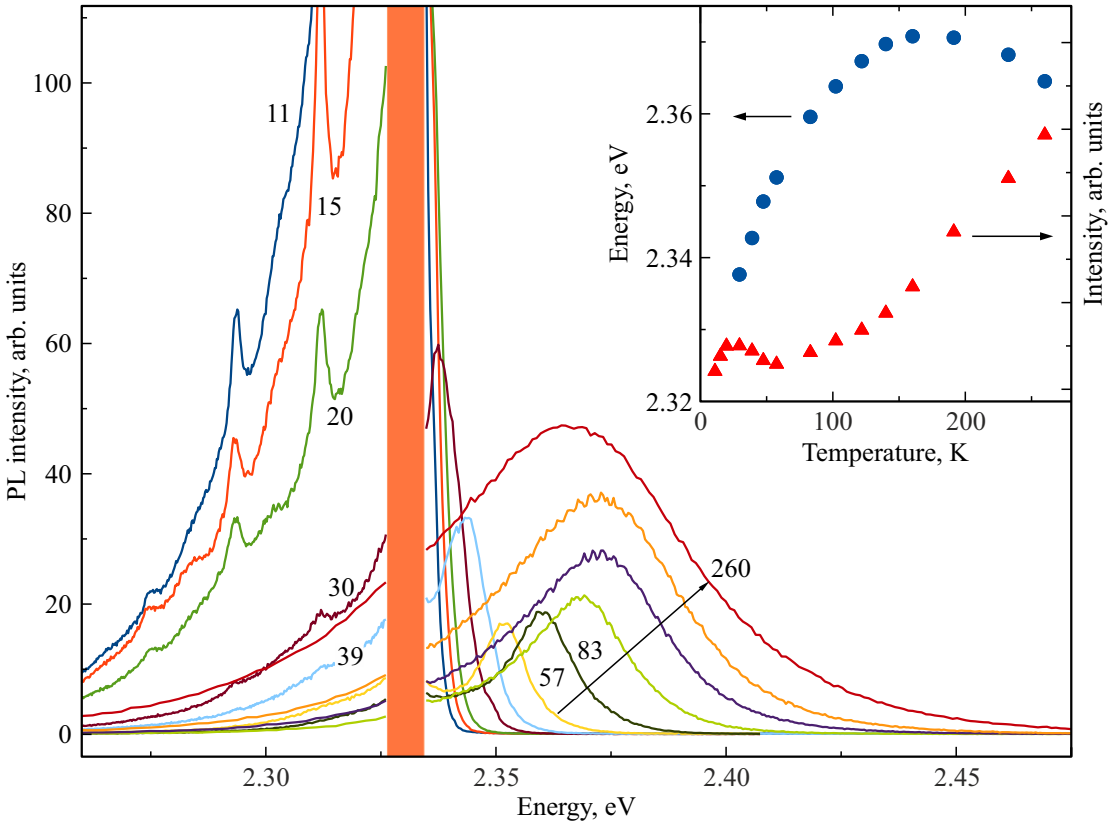

Figure 2. PL spectra of $CsPbBr_3$ nanocrystals excited by a laser with photon energy $E_{exc} = 2.33$ eV. The spectra were measured at various sample temperatures indicated near the PL lines. $P_{exc} = 1$ mW. Above the excitation energy, an ASPL band is observed. The insert shows the temperature dependence of the integral intensity of ASPL (red triangles) and the position of its maximum (blue circles).

several narrow bands are observed in the spectral range 2.32–2.39 eV. The nature of these bands is currently unclear and requires a separate study. The small full width at half maximum (less than 10 meV) of the bands indicates a narrow size distribution of the NCs. Fig. 1, *b* shows a comparison of the PL spectrum and the transmission spectrum of the sample under study. It is clearly seen that the main PL bands are observed in the region of strong absorption of the sample, which is due to the high concentration of NCs in the glass matrix. In this regard, PL detection is possible only in the back scattering geometry. Experiments have shown that even in a sample with thickness of 100 μm, PL is practically not observed in the transmission geometry.

As the temperature increases, the PL spectrum shifts to higher energies, which is determined by the behavior of the band structure of perovskites [31–35]. In the temperature range $T = 10-130$ K, the shift of the two main PL bands is well described by a linear dependence, $E = E_0 + sT$, with a slope of $s = 0.33$ meV/K for the band with energy $E_0 = 2.339$ eV and $s = 0.29$ meV/K for the band with energy $E_0 = 2.366$ eV (Fig. 1, *c*). As the temperature increases further, the shift of the bands slows down, which is associated with phase transitions in the $CsPbBr_3$ perovskite [36]. Simultaneously with the shift, the PL bands are broadened, probably due

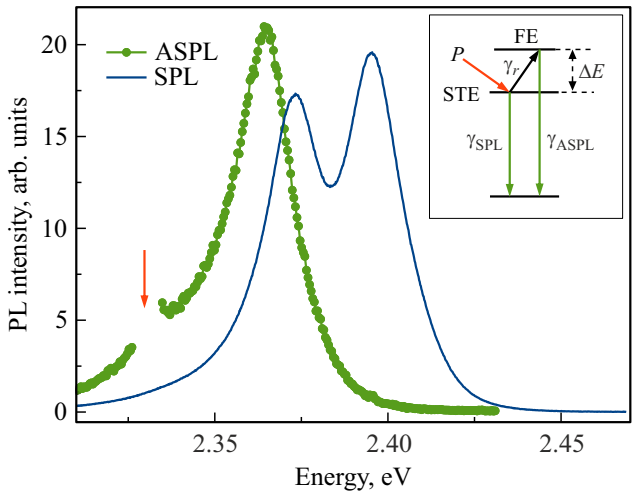

Figure 3. Comparison of PL spectra measured under non-resonant excitation ($E_{exc} = 3.06$ eV, blue solid curve) and resonant excitation ($E_{exc} = 2.33$ eV, green dotted curve). $T = 100$ K. The insert shows a diagram of the processes leading to ASPL.

to the fairly strong exciton-phonon interaction. For the high-energy band, the broadening has an approximately linear dependence with a constant $p = 64\,\mu$eV/K in the

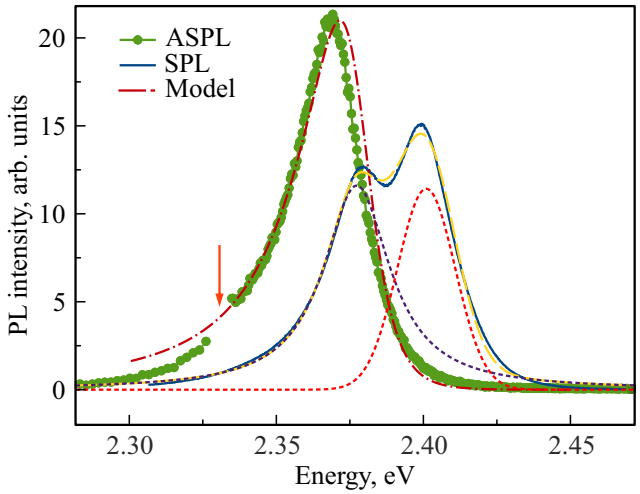

Figure 4. Simulating of ASPL spectrum by formula (6) for temperature $T = 120$ K. The green dotted curve shows the PL spectrum upon resonant excitation ($E_{exc} = 2.33$ eV). The blue solid curve shows the PL spectrum for non-resonant excitation ($E_{exc} = 3.06$ eV). The dashed curves show the decomposition of the SPL spectrum into Gaussian (right) and Lorentzian (left) contours, as well as their sum. The dashed-dotted curve shows the model contour of the ASPL. The value of the fitting parameter is $a = 50$.

temperature range $T = 10-170$ K. The linear dependence is typical for the interaction with acoustic phonons. Note that the value of the constant p is tens of times higher than the analogous constant for the well-studied semiconductor GaAs [37].

Anti-Stokes photoluminescence

When $CsPbBr_3$ nanocrystals are excited into the lower edge of the emission band by a green laser ($\lambda = 532$ nm, $E_{exc} = 2.33$ eV), the phenomenon of anti-Stokes photoluminescence (ASPL) is observed. An example of PL spectra measured under resonant excitation and different sample temperatures is shown in Fig. 2. At low sample temperatures, $T < 30$ K, only the Stokes wing of photoluminescence (SPL) with photon energy $E < E_{exc}$ is observed. The narrow peaks observed in this wing are due to phonon replicas of the resonant PL line.

As the sample temperature increases, the emission band of NCs with the photon energy $E > E_{exc}$ arises. This is the anti-Stokes PL wing. The integral intensity of this band rapidly increases with increasing temperature and becomes greater than the integral intensity of the Stokes wing already at $T > 50$ K (inset in Fig. 2). Experiments show that ASPL is observed already at a low pump power of tens of μW in a spot with a diameter of 0.05 mm, and its intensity grows linearly with increasing the pumping power. This indicates a two-stage (cascade) mechanism of ASPL excitation through real electronic states.

Model

It should be noted that the ASPL phenomenon has already been observed for perovskite NCs in other matrices [26,38–41]. The explanation of this phenomenon is based on the assumption of the existence of metastable states of excitons [self-trapped excitons (STE)] in NCs [26]. These states are lower in energy than the states of free excitons (FE). Experiments show that the STE lifetime is scattered over a large time interval from fractions up to hundreds of microseconds [42]. It is important that the STE lifetime is several orders of magnitude longer than the FE lifetime, which is fractions of a nanosecond [42,43]. Therefore, upon non-resonant optical excitation, excitons can accumulate in localized states. Moreover, they can accumulate even under resonant excitation, despite the low absorption coefficient in this region of the spectrum (Fig. 1, *b*).

Heating the NCs activates the process of thermal ejection of excitons from localized states into free ones, from which they radiate quickly. Due to the large difference between the lifetimes of free and localized excitons, ASPL can be observed even when the sample is only slightly heated, when $kT \ll \Delta E$, and the exciton thermal ejection rate is still low. Here ΔE is the energy gap between the localized and free states of excitons. This is the basis of a simple model sufficient for description of the ASPL It is shown schematically in the insert of Fig. 3.

The principle of describing the ASPL is as follows. The population dynamics of localized states, n_{STE}, is determined by the creation of excitons due to optical pumping at a rate of P, by their radiative recombination at a rate of γ_{SPL}, and by ejection of the excitons into to the level FE with rate γ_r. The balance equation has the form

$$\frac{dn_{STE}}{dt} = P - (\gamma_{SPL} + \gamma_r)n_{STE} = 0. \qquad (1)$$

Here, it is taken into account that the derivative is equal to zero under stationary pumping. It is assumed that the rate of exciton transitions to the FE level is determined by the thermal activation process

$$\gamma_r = \gamma_{r0} \exp\left[-\frac{\Delta E}{kT}\right]. \qquad (2)$$

Equations (1) and (2) make it possible to determine the temperature dependence of the Stokes wing of the PL from localized states (the Arrhenius formula)

$$I_{SPL} = \gamma_{SPL} n_{STE} = \frac{P}{1 + a \exp\left[-\frac{\Delta E}{kT}\right]}, \qquad (3)$$

where $a = (\gamma_{r0}/\gamma_{SPL})$. The population of the free exciton states, n_{FE}, is determined by the balance equation:

$$\frac{dn_{FE}}{dt} = \gamma_r n_{STE} - \gamma_{ASPL} n_{FE} = 0. \qquad (4)$$

As a result, the intensity of the anti-Stokes side of PL is determined by the formula:

$$I_{\mathrm{ASPL}} = \gamma_{\mathrm{ASPL}} n_{\mathrm{FE}} = \frac{P}{1 + \left(\frac{1}{a}\right) \exp\left[\frac{\Delta E}{kT}\right]}. \qquad (5)$$

Under conditions of resonant excitation by a green laser with a fixed photon energy, $E_{\mathrm{exc}} = 2.33\,\mathrm{eV}$, the energy gap is ΔE is defined by the formula: $\Delta E = E - E_{\mathrm{exc}}$. In an ensemble of NCs, there is a spread in the energies of the states of free excitons (FE), from which the ASPL emission occurs. This spread can be modeled by analyzing the PL spectrum during its non-resonant excitation. The analysis shows that the lower-energy PL peak is well modeled by the Lorentz contour (Fig. 4) rather than the Gaussian contour, which usually describes well the inhomogeneous broadening. A possible reason for this is the presence of the so-called Urbach tail of localized states [44]. As a result, the $I_{\mathrm{ASPL}}(E)$ spectrum can be simulated by the following formula:

$$I_{\mathrm{ASPL}}(E) = \frac{P}{1 + \left(\frac{1}{a}\right) \exp\left[\frac{\Delta E}{kT}\right]} \cdot \frac{A}{1 + [(E - E_0)/(\delta E)]^2}. \qquad (6)$$

Here E_0 is the position of the maximum of the Lorentz contour, and δE is its half-width at half-maximum.

Fig. 4 shows the simulation of the ASPL spectrum by formula (6). It can be seen that the model contour reproduces well the main features of the ASPL spectrum, in particular, its shift to the red region of the spectrum and the shape of the PL band. It should be emphasized that only one fitting parameter was used in the simulation (except for the PL intensity scale factor). This means that the described model adequately describes the observed phenomenon.

Good description of the ASPL spectrum is also observed at higher temperatures of nanocrystals. With decreasing temperature, however, it worsens somewhat. In particular, the shift of the ASPL band down in energy is not completely described. In this case, the parameter a with decreasing temperature has to be increased up to $a = 100$ at $T = 40\,\mathrm{K}$. The value of the parameter a is determined by the ratio of the limiting rate of thermally stimulated ejection of excitons into free states and the rate of their recombination from localized states. Large values of this parameter are due to the low recombination rate of the localized excitons. The variation of this parameter with a change in temperature is probably associated with a shift in the energy of exciton states, as a result of which laser radiation with a fixed photon energy excites ensembles of NCs of various sizes.

Conclusion

The anti-Stokes PL effect found in this work is due to the presence of long-lived exciton states in $CsPbBr_3$ nanocrystals. The thermal ejection of excitons into free states is accompanied by their rapid recombination with emission of photons in the anti-Stokes region of the spectrum. Simple three-level model makes it possible to describe well the energy shift and the shape of the ASPL band using PL data obtained with non-resonant optical excitation.

Acknowledgments

The authors are grateful to A.Yu. Serov for his help in studying the transmission spectra.

Funding

The authors would like to thank SPbSU for the financial support under grant № 91182694.

Conflict of interest

The authors declare that they have no conflict of interest.

References

[1] X. Li, Y. Wu, S. Zhang, B. Cai, Y. Gu, J. Song, H. Zeng. Adv. Funct. Mater., **26**, 2435–2445 (2016). DOI: 10.1002/adfm.201600109

[2] S. Yakunin, L. Protesescu, F. Krieg, M.I. Bodnarchuk, G. Nedelcu, M. Humer, G. De Luca, M. Fiebig, W. Heiss, M.V. Kovalenko. Nature, **6**, 8056 (2015). DOI: 10.1038/ncomms9056

[3] P. Ramasamy, D.H. Lim, B. Kim, S.H. Lee, M.S. Lee, J.S. Lee. Chem. Commun., **52**, 2067–2070 (2016). DOI: 10.1039/c5cc08643d

[4] G.E. Eperon, S.D. Stranks, C. Menelaou, M.B. Johnston, L.M. Herz, H.J. Snaith. Energy Environ. Sci., **7**, 982–988 (2014). DOI: 10.1039/c3ee43822h

[5] L. Protesescu, S. Yakunin, M.I. Bodnarchuk, F. Krieg, R. Caputo, C.H. Hendon, R. X. Yang, A. Walsh, M.V. Kovalenko. Nano Lett., **15**, 3692–3696 (2015). DOI: 10.1021/nl5048779

[6] F.O. Saouma, C.C. Stoumpos, J. Wong, M.G. Kanatzidis, J. Jang. Nature Commun., **8**, 742 (2017). DOI: 10.1038/ s41467-017-00788-x

[7] D. Wang, D. Wu, D. Dong, W. Chen, J. Hao, J. Qin, B. Xu, K. Wang, X. Sun. Nanoscale, **8**, 11565–11570 (2016). DOI: 10.1039/c6nr01915c

[8] S. Pathak, N. Sakai, F.W.R. Rivarola, S.D. Stranks, J. Liu, G.E. Eperon, C. Ducati, K. Wojciechowski, J.T. Griffiths, A.A. Haghighirad, A. Pellaroque, R.H. Friend, H.J. Snaith. Chem. Mater., **29**, 5168–5173 (2017). DOI: 10.1021/acs.chemmater.5b03769

[9] A. Mei, X. Li, L. Liu, Z. Ku, T. Liu, Y. Rong, M. Xu, M. Hu, J. Chen, Y. Yang, M. Graetzel, H. Han. Science, **345**, 295–298 (2014). DOI: 10.1126/science.1254763

[10] A Swarnkar, V. Kumar Ravi, R. Chulliyil, M. Irfanullah, A. Chowdhury, A. Nag. Chem. Int. Ed, **54** ,15424–15428 (2015). DOI: 10.1002/anie.201508276

[11] H. Huang, B. Chen, Z. Wang, T.F. Hung, A.S. Susha, H. Zhong, A.L. Rogach. Chem. Sci., **7**, 5699–5703 (2016). DOI: 10.1039/C6SC01758D

[12] S. Pathak, N. Sakai, F.W.R. Rivarola, S.D. Stranks, J. Liu, G.E. Eperon, C. Ducati, K. Wojciechowski, J.T. Griffiths, A.A. Haghighirad, A. Pellaroque, R.H. Friend, H. J. Snaith. Chem. Mater., **27**, 8066–8075 (2015). DOI: 10.1021/acs.chemmater.5b03769
[13] L. Protesescu, S. Yakunin, O. Nazarenko, D.N. Dirin, M.V. Kovalenko. ACS Appl. Nano Mater., **1**, 1300–1308 (2018). DOI: 10.1021/acsanm.8b00038
[14] Y. Wei, Z. Cheng, J. Lin. Chem. Soc. Rev., **48**, 310–350 (2019). DOI: 10.1039/c8cs00740c
[15] B. Chen, P.N. Rudd, S. Yang, Y. Yuan, J. Huang. Chem. Soc. Rev., **48**, 3842–3867 (2019). DOI: 10.1039/C8CS00853A
[16] Z. Zhiqin, Lihong L., Y. Facheng, Jun Zhao. J. Lum., **216**, 116722 (2019). DOI: 10.1016/j.jlumin.2019.116722
[17] J. Ren, T. Li, X Zhou, X. Dong, A.V. Shorokhov, M.B. Semenov, V.D. Krevchik, Y. Wang. Chem. Eng. J., **358**, 30–39 (2019). DOI: 10.1016/j.cej.2018.09.149
[18] S. Liu, Y. Luo, M. He, X. Liang, W. Xiang. J. Europ. Ceramic Soc., **38**, 1998–2004 (2018). DOI: 10.1016/j.jeurceramsoc.2017.10.012
[19] S. Liu, M. He, X. Di, P. Li, W. Xiang, X. Liang. Ceram. Inter., **44**, 4496–4499 (2018). DOI: 10.1016/j.ceramint.2017.12.012
[20] P. Li, C. Hu, L. Zhou, J. Jiang, Y. Cheng, M. He, X. Liang, W. Xiang. Mater. Lett., **209**, 483–485 (2017). DOI:10.1016/jmatlet.2017.08.079
[21] B. Ai, Ch. Liu, Z. Deng, J. Wang, J. Han, X. Zhao. Phys. Chem. Phys., **19**, 17349–17355 (2017). DOI:10.1039/c7cp02482g
[22] B. Ai, C. Liu, J. Wang, J. Xie, J. Han, X. Zhao. J. Am. Ceram. Soc., **99**, 2875–2877 (2016). DOI:10.1111/jace.14400
[23] Y. Ye, W. Zhang, Z. Zhao, J. Wang, C. Liu, Z. Deng, X. Zhao, J. Han. Adv. Optical Mater., **7**, 1801663 (2019). DOI: 10.1002/adom.201801663
[24] S. Liu, M. He, X. Di, P. Li, W. Xiang, X. Liang. Ceram. Inter., **44**, 4496–4499 (2018). DOI: 10.1016/j.ceramint.2017.12.012
[25] E.V. Kolobkova, M.S. Kuznetsova, N.V. Nikonorov. J. Non-Cryst. Solids, **563**, 120811 (2021). DOI: 10.1016/j.jnoncrysol.2021.120811
[26] X. Ma, F. Pan, H. Li, P. Chen, C. Ma, L. Zhang, H. Niu, Y. Zhu, S. Xu, H. Ye. J. Phys. Chem. Lett., **10**, 5989 (2019). DOI: 10.1021/acs.jpclett.9b02289
[27] E.V. Kolobkova, A.A. Lipovskii, V.D. Petrikov, V.G. Melekhin. Glass Phys. Chem., **28**, 251–255 (2002). DOI: 10.1023/A:1019918530283
[28] A.A. Lipovskii, E.V. Kolobkova I.E. Yakovlev. J. Europe. Ceram. Soc., **19**, 865–869. (1999). DOI: 10.1016/S0955-2219(98)00333-1
[29] E. Kolobkova, M.S. Kuznetsova, N. Nikonorov. ACS APPL. Nano Mater., **2**, 6928–6938 (2019). DOI: 10.1021/acsanm.9b01419
[30] E. Kolobkova, Z. Lipatova, A. Abdrshin, N. Nikonorov. Optical Materials, **65**, 124–128 (2017). DOI: 10.1016/j.optmat.2016.09.033
[31] G. Mannino, I. Deretzis, E. Smecca, A. La Magna, A. Alberti, D. Ceratti, D. Cahen. J. Phys. Chem. Lett., **11**, 2490 (2020). DOI: 10.1021/acs.jpclett.0c00295
[32] B.T. Diroll, H. Zhou, R.D. Schaller. Adv. Funct. Mater., **28**, 1800945 (2018). DOI: 10.1002/adfm.201800945
[33] B.T. Diroll, G. Nedelcu, M.V. Kovalenko, R.D. Schaller. Adv. Funct. Mater., **27**, 1606750 (2017). DOI: 10.1002/adfm.201606750
[34] B. Ai, C. Liu, Z. Deng, J. Wang, J. Han, X. Zhao. Phys. Chem. Chem. Phys., **19**, 17349–17355 (2017). DOI: 10.1039/C7CP02482G
[35] O.V. Kozlov, R. Singh, B. Ai, J. Zhang, C. Liu, V.I. Klimov. Zeitschrift Fur Phys. Chem., **232**, 1495–1511 (2018). DOI: 10.1515/zpch-2018-1168
[36] S.Z. Liu, A.R. DeFilippo, M. Balasubramanian, Z.X. Liu, S.G. Wang, Y. Chen, S. Chariton, V. Prakapenka, X.P. Luo, L.Y. Zhao, J. San Martin, Y.X. Lin, Y. Yan, S.K. Ghose, T.A. Tyson. Advanced Science, **8**(18), 2003046 (2021). DOI: 10.1002/advs.202003046
[37] A.S. Kurdyubov, A.V. Trifonov, I.Ya. Gerlovin, B.F. Gribakin, P.S. Grigoryev, A.V. Mikhailov, I.V. Ignatiev, Yu.P. Efimov, S.A. Eliseev, V.A. Lovtcius, M. Assmann, M. Bayer, A.V. Kavokin. Phys. Rev. B, **104**, 035414 (2021). DOI: 10.1103/PhysRevB.104.035414
[38] A.G. del Águila, T. Thu Ha Do, J. Xing, Wen Jie Jee, J.B. Khurgin, Q. Xiong. Nano Research, **13**(7), 1962–1969 (2020). DOI: 10.1007/s12274-020-2840-7
[39] S. Zhang, M. Zhukovskyi, B. Jank?, M. Kuno. NPG Asia Mater., **11**, 54 (2019). DOI: 10.1038/s41427-019-0156-4
[40] B. J. Roman, N.M. Villegas, K. Lytle, M. Sheldon. Nano Lett., **20** (12), 8874–8879 (2020). DOI: 10.1021/acs.nanolett.0c03910
[41] W. Zhang, Y. Ye, C. Liu, J. Wang, J. Ruan, X. Zhao, J. Han. Adv. Optical Mater., **9**, 2001885 (2021). DOI: 10.1002/adom.202001885
[42] V.V. Belykh, M.L. Skorikov, E.V. Kulebyakina, E.V. Kolobkova, M.S. Kuznetsova, M.M. Glazov, D.R. Yakovlev. Nano Lett., **22**, 4583–4588 (2022). DOI: 10.1021/acs.nanolett.2c01673
[43] M.A. Becker, R. Vaxenburg, G. Nedelcu, P.C. Sercel, A. Shabaev, M.J. Mehl, J.G. Michopoulos, S.G. Lambrakos, N. Bernstein, J.L. Lyons, T. St?ferle, R.F. Mahrt, M.V. Kovalenko, D.J. Norris, G. Rainó, Al.L. Efros. Nature, **53**, 189 (2018). DOI: 10.1038/nature25147
[44] F. Urbach. Phys. Rev., **92**, 1324 (1953). DOI: 10.1103/PhysRev.92.1324